AIP | Applied Physics Letters

Diffractive intermediate layer enables broadband light trapping for high efficiency ultrathin c-Si tandem cells

Guijun Li, Jacob Y. L. Ho, He Li, and Hoi-Sing Kwok

Citation: Applied Physics Letters **104**, 231113 (2014); doi: 10.1063/1.4883496
View online: http://dx.doi.org/10.1063/1.4883496
View Table of Contents: http://scitation.aip.org/content/aip/journal/apl/104/23?ver=pdfcov
Published by the AIP Publishing

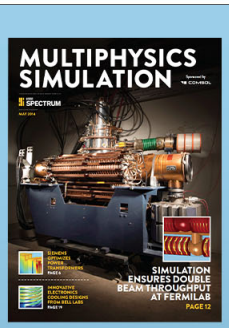

Diffractive intermediate layer enables broadband light trapping for high efficiency ultrathin c-Si tandem cells

Guijun Li,[a] Jacob Y. L. Ho, He Li, and Hoi-Sing Kwok
State Key Laboratory on Advanced Displays and Optoelectronics Technologies, Department of Electronic and Computer Engineering, Hong Kong University of Science and Technology, Clear Water Bay, Kowloon, Hong Kong

(Received 22 April 2014; accepted 2 June 2014; published online 11 June 2014)

Light management through the intermediate reflector in the tandem cell configuration is of great practical importance for achieving high stable efficiency and also low cost production. So far, however, the intermediate reflectors employed currently are mainly focused on the light absorption enhancement of the top cell. Here, we present a diffractive intermediate layer that allows for light trapping over a broadband wavelength for the ultrathin c-Si tandem solar cell. Compared with the standard intermediate reflector, this nanoscale architectural intermediate layer results in a 35% and 21% remarkable enhancement of the light absorption in the top (400–800 nm) and bottom (800–1100 nm) cells simultaneously, and ultrathin c-Si tandem cells with impressive conversion efficiency of 13.3% are made on the glass substrate. © *2014 AIP Publishing LLC*.
[http://dx.doi.org/10.1063/1.4883496]

Advanced in the thin film solar cell technologies are urgently required to continue increase the conversion efficiencies. The multijunction configurations, which are made of subcells with different semiconductor materials, have been attempted in many forms for responding to multiple light wavelengths, thus improving the conversion efficiency beyond that of single-junction solar cells.[1,2] So far, a great number of the light trapping were extensively reported to effectively enhance the light harvesting in single-junction solar cells.[3–6] To fully realize the potential of the multijunction solar cells in the class of high efficiency, light management is also an essential design consideration. A proven approach that has already been widely employed so far is to introduce an intermediate layer (IL) between the subcells to allow a better control of the light absorption in one particular subcell of which the short circuit current (J_{sc}) is the limitation of the tandem cell.[7] For example, zinc oxide (ZnO)[8] and mix-phased silicon oxide (SiO_x)[9] ILs were often implemented in the complete "micromorph" tandem solar cells to effectively enhance the light absorption of the amorphous top cell without the need of increasing the absorber thickness, therefore, light induced degradation could be reduced. These ILs, which are non-textured, usually combine the layer thickness and the refractive index mismatch to achieve the desired effect of partially reflecting the light back into the top cell. However, it is accompanied by the decrease of the light absorption in the bottom cell.[10] As a result, when a high J_{sc} is needed to meet the requirements for a high efficiency tandem cell, the bottom cell has to be made sufficiently thick for ensuring current matching, imposing the limitation of the usage of these ILs. The challenge of the light confinement in the multijunction cell is to increase the light absorption in all of the subcells simultaneously. An asymmetric intermediate reflective layer was proposed before to separate the in-coupling of the light between the top and bottom cells in an n-i-p micromorph tandem cell.[11] However, the problem of the decrease of the light absorption in the bottom cell was still not resolved. An advanced intermediate layer with the broadband light trapping capabilities is thus required and necessary. In this paper, we have met the challenge here through a diffractive intermediate layer (DIL) based on a nanoscale inverted pyramid structure, which allows for light coupling over a broader spectral range. Consequently, the improvement of absorption of the top and bottom cells can be fulfilled simultaneously, enabling a high efficiency of ultrathin a-Si/c-Si tandem solar cell.

The ultrathin amorphous/crystalline silicon (a-Si/c-Si) tandem cell is composed of a 300 nm nip a-Si top cell and an 8 μm c-Si bottom cell. The SOI wafer is used to fabricate the ultrathin c-Si bottom cell. The process began by the diffusion of 0.5 μm n^+ silicon layer and the deposition of a 250 nm aluminum. Then, an ultrathin c-Si on glass was achieved using an anodic bonding process in combination of the backside etching of the handle wafer. Next, a 12 nm p-a-Si emitter is then deposited by the plasma-enhanced chemical vapor deposition (PECVD) to form the heterojunction cell. Finally, a nip a-Si top cell is conformally deposited by the PECVD. The cell area is defined 0.1 cm^2 by the shadow mask used for the ITO antireflective coating layer sputtering. The nip a-Si top cell consists of a 25 nm n-μc-Si, a 300 nm intrinsic layer, and an 18 nm p-SiO_x layers. Two types of ultrathin a-Si/c-Si tandem cells are presented in this paper. The cells with a non-textured IL and with a DIL, which are shown schematically in Fig. 1. Alternatively, the non-textured IL is composed of 50 nm ITO and 25 nm ZnO:Al, deposited by the sputtering before the top cell deposition, the cross section of which is shown in Fig. 1(b); The nanopyramid structure is fabricated through the nanoimprinting lithography process following a anisotropic wet etching of the silicon, the 50 nm ITO, and 25 nm ZnO:Al are then conformally deposited on the structure to form the DIL [Fig. 1(d)]. The period and

[a]Author to whom correspondence should be addressed. Electronic mail: gliad@connect.ust.hk

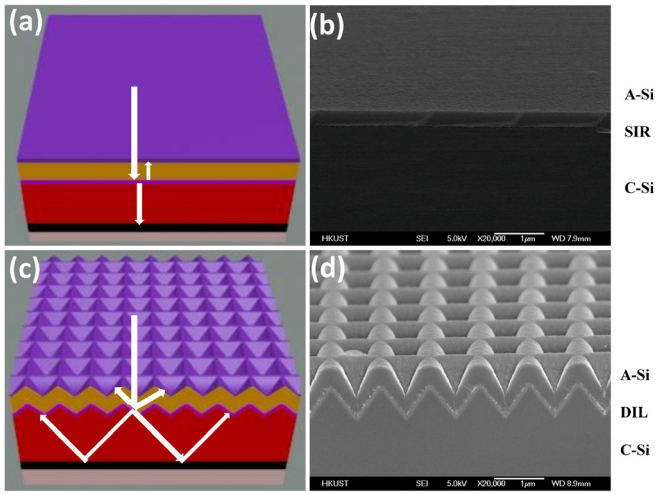

FIG. 1. Schematic of the tandem cells with different intermediate layers. (a) SIR; (c) DIL. The corresponding SEM of the SIR and DIL tandem cells are shown in (b) and (d).

height of the nanoscale inverted pyramid structure are 1000 nm and 600 nm, respectively. More details about the fabrication process can be found from our recent paper.[12] The solar cells are characterized by measuring the I–V curves under 450 W xenon lamp (Oriel, Sol2A) solar simulator in standard test conditions of simulated AM 1.5 G sunlight at 100 mW/cm^2 irradiance. The external quantum efficiency (EQE) of the tandem cells was measured using red and green bias light for the top and bottom cell, respectively.

There is only single pass for the specular incident light in the tandem cell without intermediate layer. Current densities in the top and bottom cells can be influenced through the insertion of an IL. The non-textured IL, which was also referred as symmetric or standard intermediate layer (SIR),[11] can partially reflect the light back into the top cell, often because of its low refractive index compared with the absorber layer of the top cell, but the light path length is limited to twice since there is no oblique light scattered [Figs. 1(a) and 1(b)]. In contrast to the SIR, we find that the DIL shown in Figs. 1(c) and 1(d) can effectively diffract or scatter the light into the top and bottom cells. Light trapping in the two subcell components is accomplished by the diffraction mode excited by the periodic nanopyramid structure with periodicity comparable to the wavelength of light.

Fig. 2(a) presents the EQE of the tandem cells with a SIR and a DIL, respectively. Compared to the SIR cell, manifested broadband light trapping is achieved for the DIL tandem cell. The enhancement of the light absorption in the a-Si top cell is obviously observed over a broader spectral range of interest, namely, from 400 to 800 nm. At 670 nm, the relative gain in the EQE of the top cell is 224% for the DIL, and an average gain of 35% is achieved for the top cell over the whole wavelength. However, for the bottom cell, the enhancement only occurs at the spectral region larger than 800 nm, with an average gain of 21%. For the spectral region between 550 nm and 800 nm, the DIL causes a considerable transfer of the light from the bottom cell to the top cell. In terms of the J_{sc} possible from the cells, an absolute gain of 3.1 mA/cm^2 is achieved for the top cell, whereas the gain of the bottom cell between the wavelengths of 800–1100 nm is 0.9 mA/cm^2.

It is well known that light incident on a SIR cannot couple to the guided modes. The diffractive modes can only be excited when photons interact with the nanoscale periodic structure, which could be clearly observed from the iridescent color gradient of the sample at different angles. Light trapping is fulfilled by allowing the light propagating at particular directions determined by the allowed moment changes for the incident light, the angles of which can be found from the bi-periodic grating equation.[13] Fig. 2(b) presents the diffracted angle distribution as a function of the normalized wavelength for several sets of diffractive orders using the experimentally determined value of the wavelength-dependent refractive index of the Si. For the constant lattice period of 1000 nm along x and y directions in our case, high order diffraction can only be excited at the short wavelength. At the long wavelength, both of the diffraction order and the angle decrease, and some of the modes will propagate outside the escape cone when the diffraction angle exceeds that for the total internal reflection. As the critical angles determined by the air/a-Si interface and the IRL/c-Si interface is about 15° and 33°, respectively, the first-order diffraction will propagate outside the device at the spectral range of interest and the third-order diffraction and above can be totally trapped in the bottom cell. Although the high order diffraction contributes to the total internal reflection, the intensity of which is much smaller than that of the low order diffraction, their contribution to the absorption is limited.[14] However, the light path length in the absorber layer is still enhanced by the low-order diffraction due to the oblique propagation, which is believed to be important for the absorption. The normal incident is easily visualized in

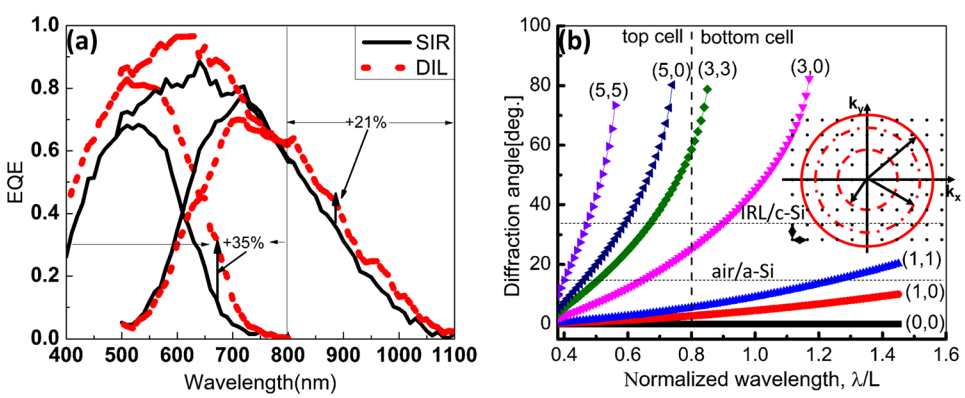

FIG. 2. (a) EQE of the SIR and DIL tandem cells; (b) diffraction angle distribution as a function of the normalized wavelength. The inset in (b) is the reciprocal grating schematic for the normal incident light.

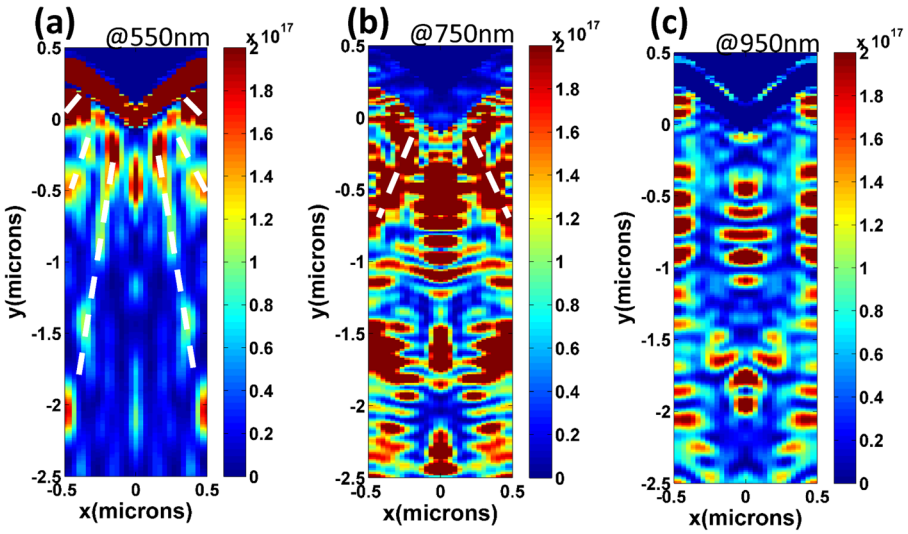

FIG. 3. FDTD simulation of the spatial distribution of the absorption in the DIL tandem cell at (a) 550 nm; (b) 750 nm; (c) 950 nm.

the reciprocal grating schematic shown in the inset of Fig. 2(b). The allowed diffraction order (m, n) within the circle is determined by the grating equation. The condition of the different wavelengths can then be represented by different circles. The smaller the circle, the larger the wavelength. When the wavelength is larger than 3.6 L (L is the lattice period), only the zeroth-order diffraction is excited. This sets the limitation for the feature size of the grating structure.

Numerical simulation based on the finite-difference time-domain (FDTD) method is used to find out the spatial distribution of the absorption. The diffraction modes can be seen unambiguous from Fig. 3 at different wavelengths, which are represented by the white dotted line in Fig. 3(a). Since most of the light is absorbed by the top cell at this wavelength, the light absorption of the bottom cell at 550 nm is not as high as that of large wavelength. Two kinds of effects are observed from the bottom cell absorption pattern at 750 nm and 950 nm. First, the number of the diffraction orders decreases with increasing the wavelength; second, the antireflection also contributes to the absorption enhancement, which is demonstrated at the specular direction.

Now returning to the experimental EQEs in Fig. 2(a). When light arrives at the nanopyramid intermediate layer interface, it will be forward or backward diffracted, respectively. As discussed above, at the medial wavelength, enhanced light absorption in the top cell benefits from the strongly coupled high order diffraction. At 670 nm where the absorption coefficient for a-Si is 5.5×10^4 cm^{-1},[15] an optical path enhancement factor of 2.8 is calculated using the Beer's law. Furthermore, it was reported that the light trapping behavior of the double sided texturing was virtually insensitive to the shape of the geometrical features,[5] which give a greatly reduced geometrical dependence. In addition to the backward diffraction, it will also be forward diffracted into the bottom cell. However, at the wavelength of the 600–800 nm, the Fresnel reflection and the backward diffraction of the nanopyramid structure will dominate and redistribute the light in the device, most of these wavelength light is therefore coupled to the top cell, light absorption in the bottom cell decreases, even though the forward diffraction occurs. At the spectral range between 800 and 1000 nm where light cannot be effectively reflected by the intermediate layer, the diffraction effect of the DIL contributes to the light absorption of the bottom cell, an average enhancement of 21% is obtained.

It is also worth noting that the enhancement of the light absorption not only arises from the diffraction effect but also ascribes to the antireflection effect of the textured top surface structure. As shown in Fig. 1(d), the conformable deposition of the intermediate layer as well as the top cell on the nanoscale pyramid structure results in a nanopyramid-like structure at the top surface, which originates from the geometrical nature of the pyramid that has a small angle of inclination.[12] The nanopyramid-like top surface provides a gradual change of refractive index from the air to the silicon, which will increase the energy entered into the device irrespective of the cell thickness. Because of the feature size of 1000 nm in our case, the antireflection effect is prominent the wavelength near 1000 nm. In order to identify the contributions from the diffraction effect of the DIL and the antireflection effect of the nanopyramid-like surface, six structures are considered and simulated. The details of these structures are summarized in Table I. The absorption spectra of the tandem

TABLE I. Six structures constructed for the simulation. The IL stands for intermediate layer. The amount of amorphous silicon in all of these cells is same.

Structure	Air/top cell surface	Top/bottom cells interface	Description
SIR	flat	75 nm IL, flat	The same as the real device
SIR&T	flat	75 nm IL, texturing	Texturing at intermediate reflector only, front surface flat
DIL	Texturing	75 nm IL, texturing	Texturing at both intermediate reflector and front surface
w/o SIR	flat	flat	Without 75 nm IL
w/o SIR&T	flat	Texturing	Without 75 nm IL, texturing at intermediate reflector only, front surface flat
DIL w/o IR	Texturing	Texturing	Without 75 nm IL, texturing at both intermediate reflector and front surface

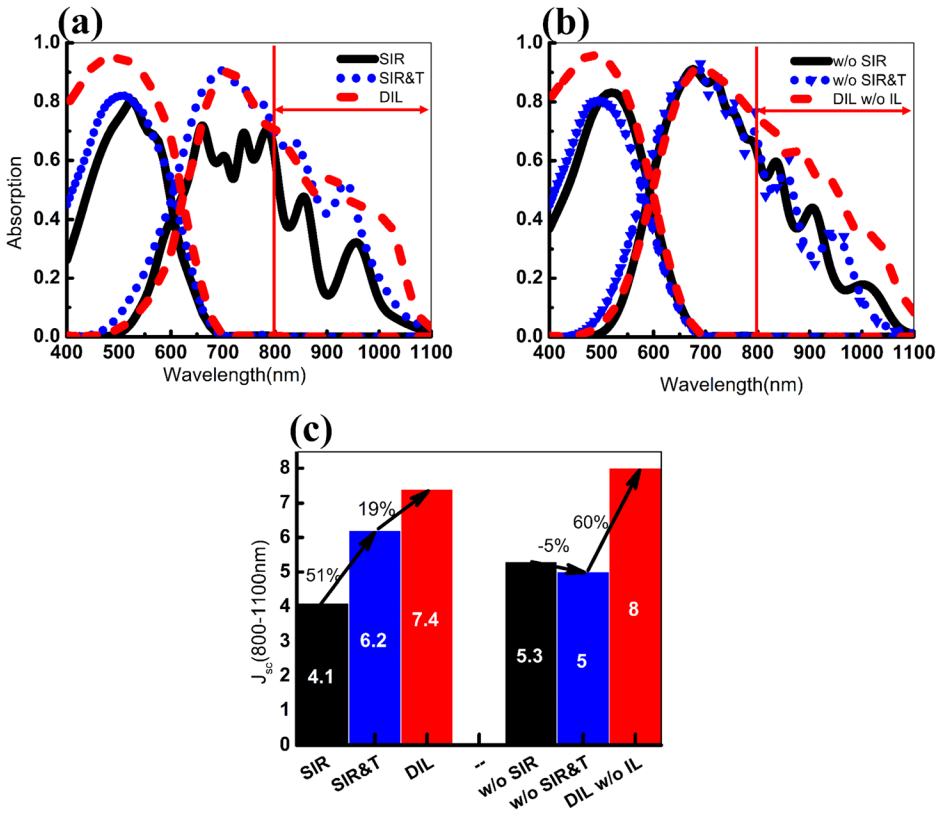

FIG. 4. (a) and (b) The simulated absorption spectra for the tandem cells with different structures; (c) the photocurrent density of bottom cells integrated from 800 to 1100 nm.

cells with different structures are shown in Figs. 4(a) and 4(b) and the corresponding short circuit current of the bottom cells (800–1100 nm) is integrated using the AM1.5 G spectrum and given in Fig. 4(c). The texturing introduced at the top/bottom cells interface can largely enhance the light absorption from 800 nm to 1100 nm for the bottom cell with respect to the SIR cell, resulting in 51% contribution of the photocurrent enhancement of the bottom cell at these spectral range. The additional introduction of the front surface texturing can only contribute to the 19% enhancement. So here we can conclude that the diffractive effect of the DIL dominates the absorption enhancement for the bottom cell (800–1100 nm) while the contribution from the antireflection effect of the nanopyramid-like surface is a little bit smaller than the former, in the case of a 75 nm intermediate layer (ITO/ZnO:Al stack) used. Surprisingly, when there is no intermediate layer inserted at the top/bottom cells interface, the texturing introduced at this interface position has no effect on the light absorption since there is no significant refractive index mismatch between the amorphous silicon and the crystalline silicon at these wavelength. However, the additional texturing at the front surface can further improve the light absorption. Because the intermediate layer is necessary for the light enhancement of the amorphous top cell, the diffractive intermediate layer based on the nanoscale geometrical structure is the best choice from the point view of the broadband light trapping, by allowing much long wavelength light to be diffracted into the bottom cell.

Although broadband light trapping is accomplished by the DIL, carefully examining the total EQE in Fig. 2(a) finds that a part of the light near the wavelength between 710 nm and 760 nm is out-coupling of the device. The observation here is in good agree with the previous result of Söderström.[11] Because the absorption coefficient is substantially small near the bandgap of the amorphous silicon, the effect is ascribed to the light reflected by the DIL will be weakly absorbed by the top cell and thus out-coupling to the escape cone of the device. The out-coupling loss can be further avoided by considering an asymmetrical grating structure.[16]

By further optimizing the deposition process of the n-μc-Si and p-SiO_x layers, remarkable conversion efficiencies of up to 13.3% have been achieved for the ultrathin tandem cells with DIL, which is a 29% higher than the SIR cells, as shown in Fig. 5. It is important to stress that the current matching of the tandem cells are all limited by the top cell, the impressive improvement of the efficiency is mainly ascribed to enhancement of the light absorption of the top cell. As can be seen from Fig. 4(a), most of the enhancement

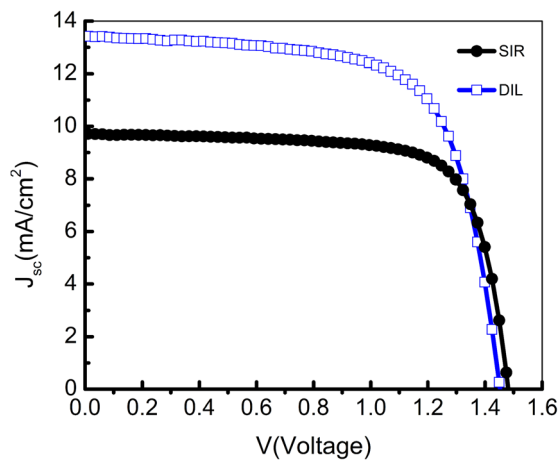

FIG. 5. IV curves of the SIR and DIL tandem cells at standard test condition.

of the top cell comes from the antireflection effect of the front surface texturing, which benefits from the conformal growth of the top cell on the nanoscale inverted pyramid structure. The texturing of the intermediate layer will have an effect on the EQE by slightly shift the absorption spectra to short wavelength. The same results can also be observed from the Fig. 4(b), but the ITO/ZnO:Al stack intermediate layer still plays a crucial role in the absorption improvement of the top cell from 500 nm to 800 nm. Further optimization of the dedicated diffraction structures in such a way as to separately maximize the subcell absorption in the spectral region of interest is required. A possible approach of continuing the progress is using the asymmetric DIL. Intuitively, in a geometric picture of the asymmetric DIL, a small feature size at the top cell/DIL interface and a large periodically grating at the DIL/bottom cell interface are preferable. Furthermore, a small feature size of the top surface will also be helpful to reduce the reflection at the short wavelength. Provided that the J_{sc} of the top cell is further improved by reducing the reflection at the top surface and the extra parasitic absorption from ITO and p-SiO_x layer, state-of-the-art efficiency above 15% can be achieved in such ultrathin c-Si tandem cell.

In conclusion, we proposed here a diffractive intermediate layer architecture for the tandem cell that enables broadband light trapping. The light absorption in the top and bottom cells is enhanced simultaneously, and impressive higher conversion efficiency of 13.3% is achieved for the ultrathin a/c-Si tandem cell. Our works suggest a viable path towards broadband light trapping of the intermediate layer structure in the tandem cell configuration.

This work was supported by the Innovation and Technology Commission of Hong Kong Government under Grant No. GHP/058/09SZ.

[1]S. P. Bremner, M. Y. Levy, and C. B. Honsberg, Prog. Photovoltaics Res. Appl. **16**, 225 (2008).
[2]J. Meier, S. Dubail, D. Discher, J. Anna Selvan, N. Pellaton Vaucher, R. Platz, C. Hof, R. Fluckiger, U. Kroll, N. Wyrsch, P. Torres, H. Keppner, A. Shah, and K.-D. Ufert, in *Proceedings of the 13th European Photovoltaic Solar Energy Conference, Nice*, 1995, pp. 1445–1450.
[3]C.-M. Hsu, C. Battaglia, C. Pahud, Z. Ruan, F.-J. Haug, S. Fan, C. Ballif, and Y. Cui, Adv. Energy Mater. **2**, 628 (2012).
[4]E. Garnett and P. Yang, Nano Lett. **10**, 1082 (2010).
[5]P. Campbell and M. A. Green, J. Appl. Phys. **62**, 243 (1987).
[6]S. E. Han and G. Chen, Nano Lett. **10**, 1012 (2010).
[7]J. Krc, F. Smole, and M. Topic, Sol. Energy Mater. Sol. Cells **86**, 537 (2005).
[8]D. Dominé, J. Bailat, J. Steinhauser, A. Shah, and C. Ballif, in *IEEE 4th World Conference on Photovoltaic Energy Conversion Conference Record* (IEEE, 2006), pp. 1465–1468.
[9]P. Buehlmann, J. Bailat, D. Dominé, A. Billet, F. Meillaud, A. Feltrin, and C. Ballif, Appl. Phys. Lett. **91**, 143505 (2007).
[10]D. Dominé, J. Steinhauser, L. Feitknecht, A. Shah, and C. Ballif, in Proceedings of the IEEE Photovoltaic Energy Conversion (2006), Vol. 3, p. 1465.
[11]T. Söderström, F.-J. Haug, X. Niquille, V. Terrazzoni, and C. Ballif, Appl. Phys. Lett. **94**, 063501 (2009).
[12]G. Li, H. Li, J. Y. L. Ho, M. Wong, and H. S. Kwok, Nano Lett. **14**, 2563 (2014).
[13]K. Johnson, Grating diffraction calculator (gd-calc) - coupled- wave theory for biperiodic diffraction gratings, 2006.
[14]C. Battaglia, C.-M. Hsu, K. Söderström, J. Escarré, F.-J. Haug, M. Charrière, M. Boccard, M. Despeisse, D. T. L. Alexander, M. Cantoni, Y. Cui, and C. Ballif, ACS Nano **6**, 2790 (2012).
[15]E. Palik, *Handbook of Optical Constants of Solids* (Academic Press, Orlando, 1985), Vol. 1, pp. 577–580.
[16]J. Gjessing, A. S. Sudbø, and E. S. Marstein, J. Appl. Phys. **110**, 033104 (2011).